

Optimal Pneumatic Actuator Positioning and Dynamic Stability using Prescribed Performance Control with Particle Swarm Optimization: A Simulation Study

Addie Irawan ^{a,1,*}, Mohd Syakirin Ramli ^a, Mohd Herwan Sulaiman ^a, Mohd Iskandar Putra Azahar ^a, Abdul Hamid Adom ^b

^a Faculty of Electrical & Electronics Engineering Technology, Universiti Malaysia Pahang, 26600 Pekan, Pahang, Malaysia

^b Faculty of Electrical Engineering & Technology, Universiti Malaysia Perlis, Pauh Putra Campus 02600 Arau, Perlis, Malaysia

¹ addieirawan@ump.edu.my

* Corresponding Author

ARTICLE INFO

ABSTRACT

Article history

Received April 12, 2023

Revised May 13, 2023

Accepted May 30, 2023

Keywords

Pneumatic actuator;
Prescribed performance control;
Swarm intelligence;
Metaheuristic

This paper introduces an optimal control strategy for pneumatic servo systems (PSS) positioning using Finite-time Prescribed Performance Control (FT-PPC) with Particle Swarm Optimization (PSO). Pneumatic servo systems are widely used in industrial automation, as well as medical and cybernetics systems that involve robotics applications. Precision in pneumatic control is crucial not only for the sake of efficiency but also safety. The primary goal of the proposed control strategy is to optimize the convergence rate and finite time of the prescribed performance function in error transformation of the FT-PPC, as well as the Proportional, Integral and Derivative (PID) controller as the inner-loop controller for this system. The study utilizes a dynamic model of a pneumatic proportional valve with a double-acting cylinder (PPVDC) as the targeted plant and performs simulations with a multi-step input trajectory. This offline tuning method is essential for such nonlinear systems to be safely optimized, avoiding major damage to the real-time fine-tuned works on the controller. The results demonstrate that the proposed control strategy surpasses the performance of FT-PPC with a PID controller alone, significantly improving the system's performance, including suppressing overshoot and oscillation in the responses. Further validation through the actual system of PPVDC using the fine-tuned values of FT-PPC and PID with PSO is a future task and more challenging to come, as hardware constraints may vary with different environments such as temperatures.

This is an open-access article under the [CC-BY-SA](https://creativecommons.org/licenses/by-sa/4.0/) license.



1. Introduction

Pneumatic servo systems (PSS) are crucial actuators used in various applications, such as industrial automation, biological inspired systems, and manufacturing processes. In industrial automation, PSS is widely used in mass production line machines like pick-and-place machines, hammer peening [1], winder machines [2] and pressing processes [3]. For biological-inspired systems, many works are related to robotics systems for rehabilitation, wearables, and mobile robot systems for various applications. For example, Wu *et al.* developed a soft finger inspired by the

multi-knuckles of humans based on pneumatic actuation. They proposed a combination of three independent-actuated segments to enable dexterous manipulation as compared to conventional soft finger design approaches [4]. A teleoperation system using a haptic glove unit by [5] is another example of PSS application in a wearable system. The system introduced a self-sensing method in human-machine interfaces to achieve accurate interaction motion. Moreover, a micro-robot by Jin *et al.* is an example of PSS in bio-inspired systems. The system is inspired by the biological structure of caterpillars and is designed by integrating two types of ultra-stretchable bionic sensors on a dual air-chamber pneumatic network structure and four triboelectric nanogenerator tactile sensors (TTSS) based on functional liquid metal (FLM) with thorny-structured bionic whiskers to realize self-powered tactile sensors [6].

The primary challenge in PSS is still on the individual actuator control, especially in positioning and internal stability. Designing a high-performance controller for these actuators remains challenging due to the system's high nonlinearity and parameter variations. Additionally, it becomes more challenging when dealing with long-stroke configurations due to the system's nonlinear dynamics proportional to the cylinder's wide operation range. As a result, controlling the plant becomes difficult, and an efficient controller is challenging to design. There have been numerous efforts to improve control systems for pneumatic actuators, with a particular focus on controlling the position of the rod-piston. These efforts include the use of control theories through numerical methods [7], [8], integration with intelligent systems [8], [9] and parameter designed using computational methods [10], [11]. Moreover, some control strategy approaches have been done by engineers and researchers to cater to the PSS issues, such as integration controllers' methods or hybrid techniques, as done in [12], [13]. The other integration methods include cascading control, adaptive control, intelligent control, and optimal control using computational methods [14]-[17]. The Proportional, Integral, and Derivative (PID) control system is a classical control system that is commonly deployed and becomes standard in most systems. However, it has limitations in providing efficient control for a nonlinear system such as PSS. PSSs suffer from various drawbacks such as low rigidity caused by air compressibility, delay in pressure response, fluctuations in frictional force between pistons and sliding parts within cylinders, and changes in air temperature. The effectiveness of conventional control such as PID and its adaptive versions depends on the magnitude of nonlinearity in the PSS [18]. Only when the nonlinearity is negligible, these techniques can be effective. Additionally, this type of controller requires optimum fine-tuning in its design and is fragile to different disturbances. Therefore, a few researchers have approached optimization methods through either adaptive techniques, integration techniques with conjunction controllers, or computational methods to determine the optimum design parameter values for the main controller as reported in [19], [20].

The conjunction control system approach can be improved to enhance the robustness of complex systems. In addition to the cascaded control methods, the prescribed performance control (PPC) approach, introduced by Bechlioulis *et al.* uses output constraints approach to ensure the system output converges to a prescribed narrow area, with minimal overshoot and steady-state error [21]. This approach has the potential to improve the deployment of closed-loop control systems, especially those that involve conventional control systems such as PID controllers. Some researchers have enhanced the conjunction control system by transforming its error, making it more practical and dynamic for real-time control systems, as demonstrated in studies [22]-[25]. However, fine-tuning its parameters is still necessary to optimize its potential.

The use of computational intelligence integrated with optimization strategies is becoming increasingly popular as a solution to the complexity, nonlinearity, and other difficulties encountered in practical engineering problems, such as pneumatic systems, for improving the performance of control systems. The function approximation-based intelligent design strategy is widely recognized as an effective way to deal with unknown nonlinearities and uncertainties. Metaheuristic approaches also play a significant role in machine learning, providing excellent results. These approaches allow for the efficient optimization of parameters of interest, leading to good generalization. For decades,

various metaheuristic approaches have been introduced, including Evolutionary Algorithms (EA), Swarm Intelligence (SI), Physic-Based Algorithms (PBA) [26], and Human-Based Algorithms (HBA). EA, for example, generates new offspring that inherit characteristics from their parents, mimicking the evolutionary process. One notable example of an EA-based optimization method is the Genetic Algorithm (GA) [27] which has been proven to be highly effective in various fields, such as transportation/mobile system [28], [29], robotics/automation [30], [31], time series etc. Other examples of EA-based optimization methods include Differential Evolution (DE) [32] and Evolutionary Programming [33]. In contrast, SI algorithms mimic the unique behaviour of animals or insects, with Particle Swarm Optimization (PSO) [34] being the first to emerge. Other SI-based optimization methods include Ant Colony Optimization (ACO) [35], Artificial Bee Colony algorithm (ABC) [36], Grey Wolf Optimizer (GWO) [37], Moth Flame Optimizer (MFO) [38], Barnacles Mating Optimizer (BMO) [39] and one the latest is Evolutionary Mating Algorithm (EMA) [40]. PBA is exemplified by the Gravitational Search Algorithm (GSA) [41], which is based on Newton's law of gravity, while the Harmony Search Algorithm (HSA) [42] is based on the process of jazz musicians. Both GSA and HSA have been successfully applied in various fields to address optimization tasks. The implementation and deployment of optimization algorithms in real-time remain a significant challenge, particularly for systems equipped with limited processing units that require fast responses. Researchers have recently proposed approaches for real-time control and measurement using computational intelligence, but their deployment is limited to systems that use major high-speed computer systems that run in parallel with other tasks, such as image processing, traffic large signals, trajectory planning, and data communications [43]-[46]. Most driven systems fine-tuned and optimized for automation units, such as actuator and motor control, are generally done through offline strategies, as these units require robust continuous control systems and highly fast response rather than learning systems during real-time operation. However, some efforts have been made to provide a learning system in actuating control modules independently, as reported in [47]-[49]. Still, there is a lot of work to be done, especially in identifying and modeling the plant for the model-reference of the controller and pre-tuning works through simulations.

Therefore, the objective of this study is to contribute to the field of fine-tuned control system design for PSS's rod-piston positioning. To achieve this, the study uses the PSO algorithm through an offline approach as a pre-fine-tuned task to design the parameters for both cascaded control systems, FT-PPC and PID. Precise rod-piston positioning is crucial not only for the physical rod-piston but also for the overall internal system of PSS. PSO is an established and widely used swarm intelligence system in engineering applications, including fine-tuned control systems. The targeted PSS for this study is a Proportional Valve with a Double-Acting Cylinder (PPVDC) [50]. The multi-step input trajectory of the rod-piston displacement was generated to the targeted system with PSO optimization. The paper is organized as follows: [Section 2](#) provides an overview of the mathematical modelling of the PPVDC. [Section 3](#) describes the prescribed performance control strategy with PID in detail. [Section 4](#) discusses the PSO algorithm and its application to FT-PPC-PID. The analysis and performance of the FT-PPC-PID controller with PSO optimization are discussed in [Section 5](#) and are compared with FT-PPC-PID and PID alone on the same PPVDC model plant. Finally, [Section 6](#) draws the conclusion.

2. Overview of the PPVDC Model

For this study, the model plant transfer function was obtained from the dynamic model of the Proportional Valve with a Double-Acting Cylinder (PPVDC) on the Tri-finger Pneumatic Grasper (TPG) robot platform [51], [52] as shown in [Fig. 1](#). The proportional control valve regulates the air passage to the cylinder. The model primarily focuses on three sections: cylinder dynamics, friction dynamics, and valve dynamics. To obtain the motion equation for the pneumatic actuator's cylinder dynamics (1).

$$\ddot{x}_{rp} = \frac{A_1 P_1 - A_2 P_2 - (F_f - F_L)}{M_p + M_L} \quad (1)$$

where \ddot{x}_{rp} is the acceleration condition of the pneumatic rod-piston, while A_1, A_2 represents the nozzle area of each pneumatic cylinder rod-piston chamber. Moreover, P_1, P_2 here are the cylinder chambers' absolute pressures and other properties like F_f, F_L, M_p and M_L are internal forces and masses of the pneumatic cylinder system in which was detailed in [53].

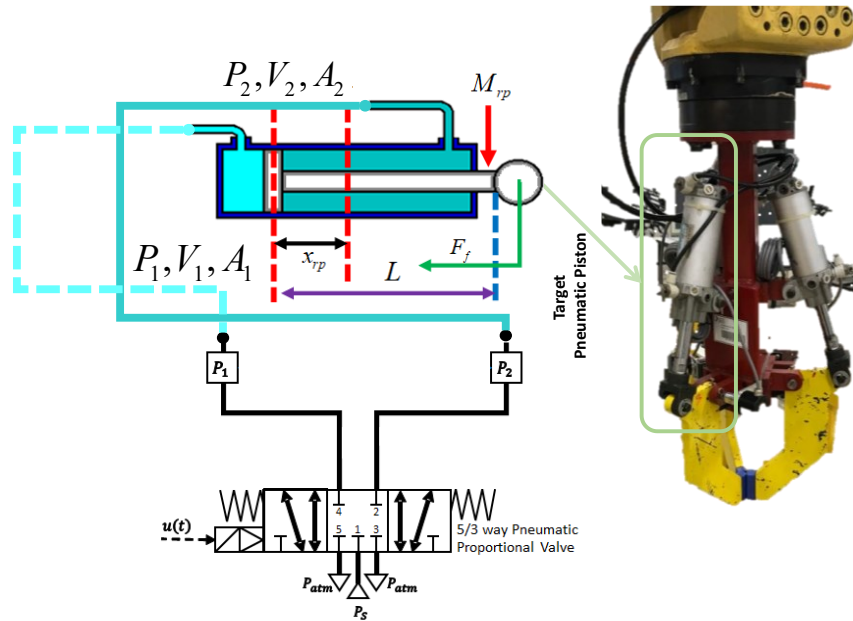


Fig. 1. PPVDC hardware schematic with TPG [14]

On the friction's dynamics, the LuGre friction model was used which can be generally expressed in (2).

$$F_f = \lambda_0 \zeta + \lambda_1 \dot{\zeta} + \lambda_2 \dot{x}_{rp} \quad (2)$$

where λ_n with $n = 1, 2, 3$. are the coefficients of the friction's dynamics where $n = 1$ denotes the spring bristle factor, $n = 2$ denotes damping bristle factor and viscous friction factor with $n = 3$, further detail regarding this function can be find in [14]. Since the temperature is negligible, the differential equation for both pressure chambers is computed as follows under the adiabatic assumption [12].

$$\dot{P}_{i(i=1,2)} = \frac{kRT\dot{m}_{i(i=1,2)}}{V_{0i(i=1,2)} + A_{i(i=1,2)}(0.5L \pm x_{rp})} - \frac{kP_{i(i=1,2)}A_{i(i=1,2)}\dot{x}_{rp}}{V_{0i(i=1,2)} + A_{i(i=1,2)}(0.5L \pm x_{rp})} \quad (3)$$

where x_{rp} and L are the displacement and length of the pneumatic actuation stroke, respectively. The heat capacity ratio of the air medium, the universal gas constant, and the air absolute temperature are represented by k, R and T , respectively. The mass flow rate denotes by $\dot{m}_{i(i=1,2)}$ and the dead volume of pressurized gas confined in the connecting tube between the pneumatic valve and the pneumatic cylinder is referred to as $V_{0i(i=1,2)}$. The valve dynamics, on the other hand, were derived directly from the orientation of the valve spool (x_{pv}), which is proportional to the voltage input (u) and valve gain (k_{pv}). This relationship can be expressed according to the Karpenko and Sepehri [54] in (4)-(5).

$$\dot{x}_{pv} = -\frac{x_{pv} + k_{pv}u}{\tau} \quad (4)$$

$$u = \frac{A_{pv}}{\omega k_{pv}} \quad (5)$$

where the τ is a valve spool time constant and ω is the valve orifice area gradient. Moreover, the valve orifice effective area are denoted as A_{pv} [14]. The standard length of the connecting tube in the model was assumed to be short enough to be neglected as a significant contributor to the time delay in the PPVDC system. The overall structure of the PPVDC model is illustrated in Fig. 2. The parameter values, including the dead-zone parameters of the PPVDC valve and its cylinder frictional force parameters, were identified in previous work [12]. These parameters were obtained using the procedures reported in [55].

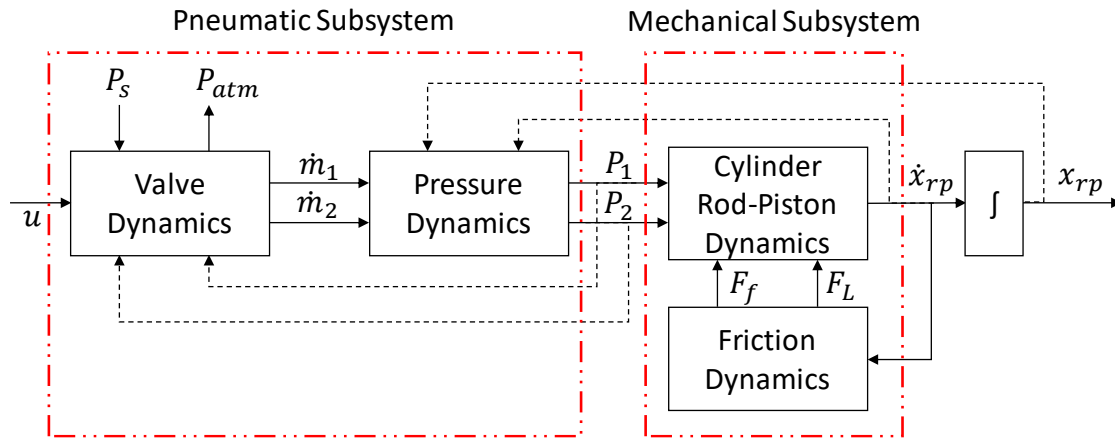


Fig. 2. Mathematical model of the PPVDC structure [14]

3. Controller Design

In this study, the formulated finite-time prescribed performance control is designed with proportional, integral, and derivative (PID) control for rod-piston positioning of the PPVDC plant. The prescribed performance function (PPF) was improved with finite-time elements according to the drawbacks found in the original form of PPC introduced by [21].

3.1. Finite-time Prescribed Performance Function

The idea of adding finite-time in conventional PPC design emerged due to the two notable deficiencies noticed in the performance function of conventional PPC [21]. These can be expressed in (6).

$$\rho(t) = (\rho_0 - \rho_\infty)e^{-ht} + \rho_\infty \quad (6)$$

Where ρ_0 denotes the initial transient state tracking error. The maximum permissible range of the $e(t)$ boundary, represented as ρ_∞ , is reached at $\rho_0 > \rho_\infty > 0$. According to the [21], the concrete convergence time was unprescribable when $\rho(t)$ and $t \equiv \infty$ as reaches the stability boundary ($\rho(\infty)$). Additionally, the constant exponential convergence rate (h) is one of the limitations in manipulating the PPF in practical use. Hence, to address these drawbacks, this study has introduced an improved PPF with finite-time components that can be expressed in (7).

$$\rho(t) = (\rho_0 - \rho_\infty)e^{-\frac{t^2}{2\left(\frac{t_e}{2}\right)^2}} + \rho_\infty \quad (7)$$

3.2. Error Transformation

An error transformation approach is introduced to convert origin-constrained tracking error, $e(t)$, into an unconstrained one. This is done to emphasize the relationship between two variables, $\rho(t)$ and $e(t)$ by using the formula in (8).

$$e(t) = \rho(t)S(\varepsilon) \quad (8)$$

where

$$S(\varepsilon(t)) = \frac{\bar{\sigma}e^{\varepsilon(t)} - \underline{\sigma}e^{-\varepsilon(t)}}{e^{\varepsilon(t)} + e^{-\varepsilon(t)}} \quad (9)$$

and the purpose of developing $\varepsilon(t)$ is to enhance the functionality of $S(\varepsilon)$. The $|e(t)| < \rho(t), \forall t \geq 0$ is achieved due to $S(\varepsilon)$ being strictly monotonic increasing. Conversely, defining $\rho(t)$ can regulate the behavior of both transient responses and steady error inputs of the closed-loop controller. The inverse transformation function for the bounded $\varepsilon(t)$ can be expressed in (10).

$$\varepsilon(t) = S^{-1}\left(\frac{e(t)}{\rho(t)}\right) = \frac{1}{2} \ln\left(\frac{\psi(t) + 1}{1 - \psi(t)}\right) \quad (10)$$

The control objective is to constrain $\varepsilon(t)$ in order to create precise positioning control. $\varepsilon(t)$ is a newly transformed tracking error variable, and $S^{-1}(\bullet)$ represents the inverse function of $S(\varepsilon)$. The normalized error, $\psi(t) = \frac{e(t)}{\rho(t)}$, is valid only when $|\varepsilon(0)| < 1$. $\psi(t)$ satisfies $-1 < \psi(t) < 1$ when $\varepsilon(t) \neq \infty$, and the predefined bound of PPF [35] is guaranteed as long as $\varepsilon(t)$ is constantly bounded. Note that the boundary value surrounding $\varepsilon(t)$ has no effect on the reaction $e(t)$. Rather, it is determined by (8) using the predefined $\rho(t)$. As a result, the control input of the PID controller can be expressed in (11).

$$u(t) = K_p\varepsilon(t) + K_i \int \varepsilon(t)dt + K_d \frac{d}{dt}\varepsilon(t) \quad (11)$$

where $\{K_p, K_i, K_d\} > 0$ the design parameters. The overall control architecture is shown in Fig. 3.

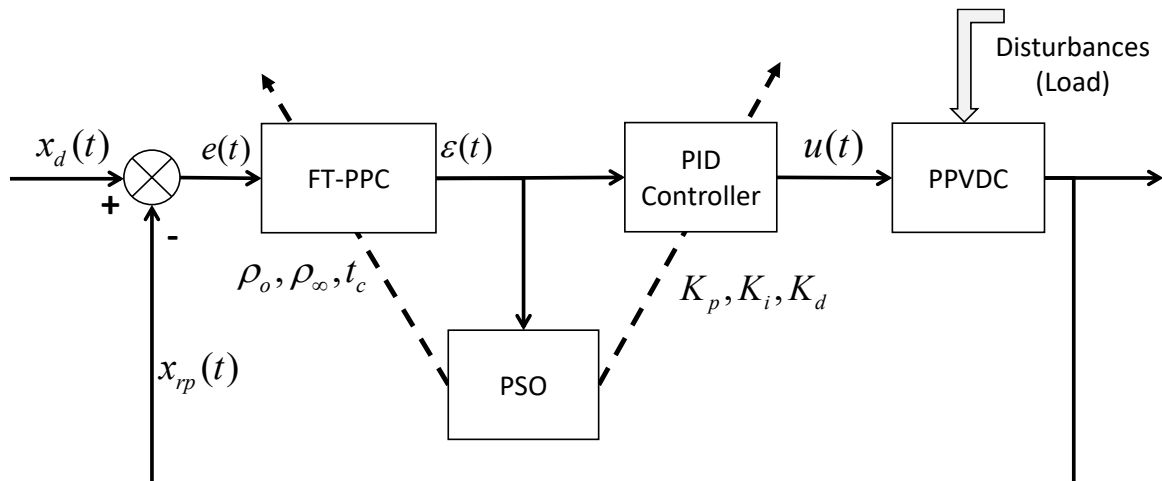


Fig. 3. FT-PPC and PID with PSO control architecture overview for PPVDC rod-piston positioning

4. Controller Optimization Using Particle Swarm Optimization

The parameters of the decay smooth function and the PID controller in PPF are optimized simultaneously using the PSO algorithm. PSO is a type of SI algorithm introduced by Kennedy and Eberhart in 1995 [34], inspired by the social and cooperative behaviors of swarms of birds or fish in

search of their needs. The state feedback control for FT-PPC-PID can be expressed as a single entity. The overall state feedback control for FT-PPC-PID can be expressed in the form of $\Lambda := [K_p \ K_i \ K_d \ \rho_o \ t_c \ \rho_\infty]^T \in \mathcal{R}^6$.

Problem 1: The optimal solution $\Lambda^* \in \mathcal{R}^6$ such that

$$\Lambda^* := \arg \min_{\Lambda} J(\Lambda). \quad (12)$$

where J is a cost function calculated from the Mean Absolute Error (MAE) percentage of each iteration (k) of $\varepsilon(t)$ in (13).

$$J(\Lambda, k) := 100|\varepsilon(t)|. \quad (13)$$

The optimization process starts by randomly inserting the number of agents (M) with random position $p_i \in \mathcal{R}^{1 \times N}$ and velocity $q_i \in \mathcal{R}^{1 \times N}$ in the search area dimension (N). In each k , each particle or agent (i) is updating its position according to the global best position. Each agent's position corresponds to specific rewards measured by the selected fitness function (f_{fit}) value. Function in (13) will continuously update the current agent's velocity with reference to those reward values. The updating function can be expressed in (14).

$$q_i(k+1) = \omega q_i(k) + \eta_1 r_1 (p_{best_i} - p_i(k)) + \eta_2 r_2 (g_{best} - p_i(k)) \quad (14)$$

where cognitive represented by $\eta_1, \eta_2 \in \mathcal{R}$ and social learning represented by $r_1, r_2 \in \mathcal{R}$ are the real numbers that generated randomly between 0 and 1. The parameter $\omega \in \mathcal{R}$, on the other hand, is the inertia function that balances local and global search capabilities. The best position of current agents and the best solution among the current agents are represented by p_{best_i} and g_{best} , respectively. Using the velocity formula (14), the agent's position is subsequently updated using the given function in (15).

$$p_i(k+1) = p_i(k) + q_i(k+1). \quad (15)$$

In each iteration, the value ω is updated to ensure that it decreases linearly from its maximum weight, $\omega_{max} \in \mathcal{R}$, to its minimum weight, $\omega_{min} \in \mathcal{R}$. The scenario can be expressed using function in (16).

$$\omega = \omega_{max} - \left(\frac{\omega_{max} - \omega_{min}}{T_{max}} \right) T \quad (16)$$

The maximum number of iterations is represented by $T_{max} \in \mathcal{R}$, and the current iteration number is represented by T . Suppose that at the last iteration, the optimum location of the agent, $p^* \in \mathcal{R}^{1 \times N}$, is found, such that it yields the minimum value of the fitness function. In that case, all agents are expected to converge to this location, implying that:

$$p^* := \arg \min_{p_i} f_{fit}, \forall i. \quad (17)$$

To explain the approach used in this study in applying the PSO algorithm to solve **Problem 1**, the algorithm's steps are presented below, with reference to Fig. 3.

- Step 1:** The initial gains for the PID = $\{K_p, K_i, K_d\}$ and FT-PPC = $\{\rho_o, t_c, \rho_\infty\}$ are arbitrarily selected which can be represented as tunable gain Λ .
- Step 2:** First, define the search area for the agents, along with the number of particles and parameters. Afterwards, the initial position of all agents is randomized within the specified search area. Continuing with that, the fitness function's value for each position is evaluated. As the optimization problem is to solve **Problem 1**, whereby $f_{fit} = J$, as given by (13), is a suitable candidate for the fitness function.

- Step 3:** For every k , the velocities (14) and positions (15) of the agents are updated until T_{max} is reached, and all agents are expected to converge to the optimal position, p^* , which corresponds to the optimal solution for (13).
- Step 4:** Finally, assign the optimal gain parameters, $\Lambda^* = p^*$, and verify the performance in the actual system model. If the results are unsatisfactory, repeat **Step 2**.

5. Results and Discussions

The PSO-FTPPC-PID controller was tested with the PPVDC dynamic model using the SIMULINK MATLAB® environment. A comparison was made between the fine-tuned PID controller and FT-PPC. The system was subjected to an external disturbance of 5kg, and a multi-step input trajectory with retract-extend of half rod–piston (0–0.15 m) of a finger of TPG was used on the piston to observe the controller's response. The analysis aimed to verify the precision of PPVC rod-piston positioning and the stability of the internal pneumatics system. The analysis aimed to verify the precision of PPVDC rod-piston positioning and the stability of the internal pneumatics system. The main reason for this comparison and analysis is to verify the effectiveness of optimizing FTPPC-PID using PSO as compared to the FTPPC-PID bang-bang tuning. On the other hand, comparison with PID controller is to see the effectiveness of FTPPC-PID in enhancing the PID performance in prescribing error tracking performances. The fine-tuned values for the PID and FTPPC-PID controllers and PSO are shown in Table 1. For the case of PSO-FTPPC-PID, the optimum fine-tuned values were achieved whenever $J \rightarrow 0$ as can be depicted in Fig. 4 whereby $J = 0.007\%$ at $k = 0$ starting to $J = 0.00357\%$ at $k = 100$.

Table 1. Controller Parameters

Controller	PID			FT-PPC		
	P	I	D	ρ_0	t_c	ρ_c
PID	40	1.8	0.3	NA	NA	NA
FT-PPC-PID	65	0.5	0.8	1	0.2	0.15
PSO-FTPPC-PID	42.3723	0.6200	0.4359	5.5531	0.3997	5.2985

Fig. 5 illustrates the performance comparison between the controllers. The results demonstrate that the PSO-FTPPC-PID achieved the desired position quickly, with very low overshoot and time lag compared to the FTPPC-PID. Conversely, the PID controller's performance was inferior, exhibiting high oscillation and a settling time lag of around 0.8 seconds, in contrast to the PSO-FTPPC-PID. A zoom-in view of the results for a sample period of 1-2 seconds, as depicted in Fig. 5(b), further highlights these distinctions. Despite the presence of payloads, the PSO-FTPPC-PID effectively handled oscillation, nearly 0% compared to the FTPPC-PID, and significantly outperformed the PID controller in positioning the PPVDC rod-piston. These results also validate that the error transformation by FTPPC can prescribe between the decay smooth function boundaries, as demonstrated in Fig. 6. Moreover, Fig. 6(b) shows that the PSO-FTPPC-PID controller can effectively suppress the overshoot that occurs during transient step inputs by adjusting the boundaries and PID gain tuning, in contrast to the FTPPC-PID controller alone. This is evidenced in the error transformation results between 0.99 and 1.06 seconds, as depicted in Fig. 6(b) and can be compared with Fig. 5(b).

The PSO-FTPPC-PID controller also effectively reduces oscillations in the cylinder chambers, which are caused by changes in rod-piston displacement, as shown in Fig. 7 and Fig. 8 for Pressure 1 and Pressure 2 respectively. The PPVDC rod-piston movement can be controlled more precisely with a slightly higher pressure of about 0.2Pa compared to FTPPC-PID, and minor overshoots occur only during the first change of displacement (refer to Fig. 5). Fig. 7(b) provides a clearer view of this phenomenon for the 1-2 second sample interval. In contrast, PID exhibits a high frequency of oscillations after a period of displacement change, as depicted in Fig. 7(b), which leads to difficulties in achieving the desired position, as shown in Fig. 5. The same pattern is observed in the performance

of Pressure 2, albeit at the opposite value level, as demonstrated in Fig. 8. The situation is more evident in the 1-2 second sample interval, as shown in Fig. 8(b).

Fig. 7 and Fig. 8 demonstrate that classical PID produces the highest overshoot and internal vibrations in both pressure chambers, resulting in a single spike at each change in rod-piston displacement as shown in Fig. 5. In contrast, PSO-FTPPC-PID can reduce this overshoot in both pressure chambers, leading to sustained high pressures in Pressure 1 and vice versa in Pressure 2, resulting in an average displacement overshoot of almost 0.04% as depicted in Fig. 5. The oscillation and overshoot in the cylinder chambers have also affected the velocity performance, which seems to be proportional to the internal frictional forces as shown in Fig. 10. The proposed PSO-FTPPC-PID and classical FTPPC-PID exhibited significantly better performance than PID control, which experienced massive spikes and high oscillation in PPVDC rod-piston speed.

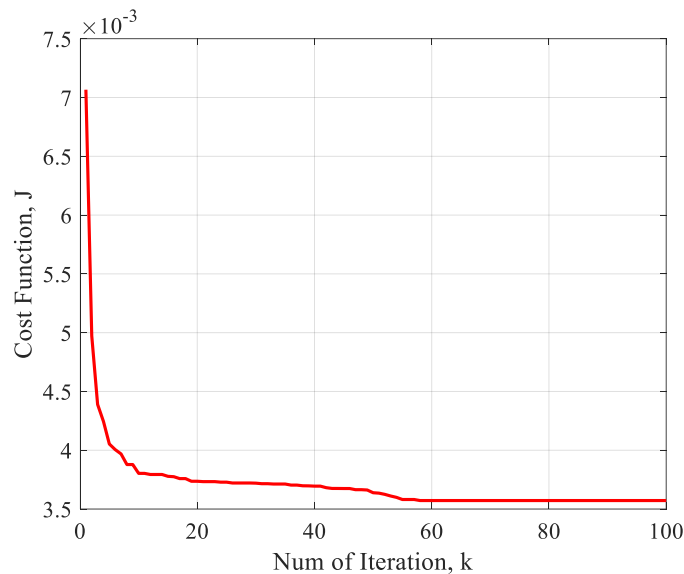


Fig. 4. Cost function (J) convergence

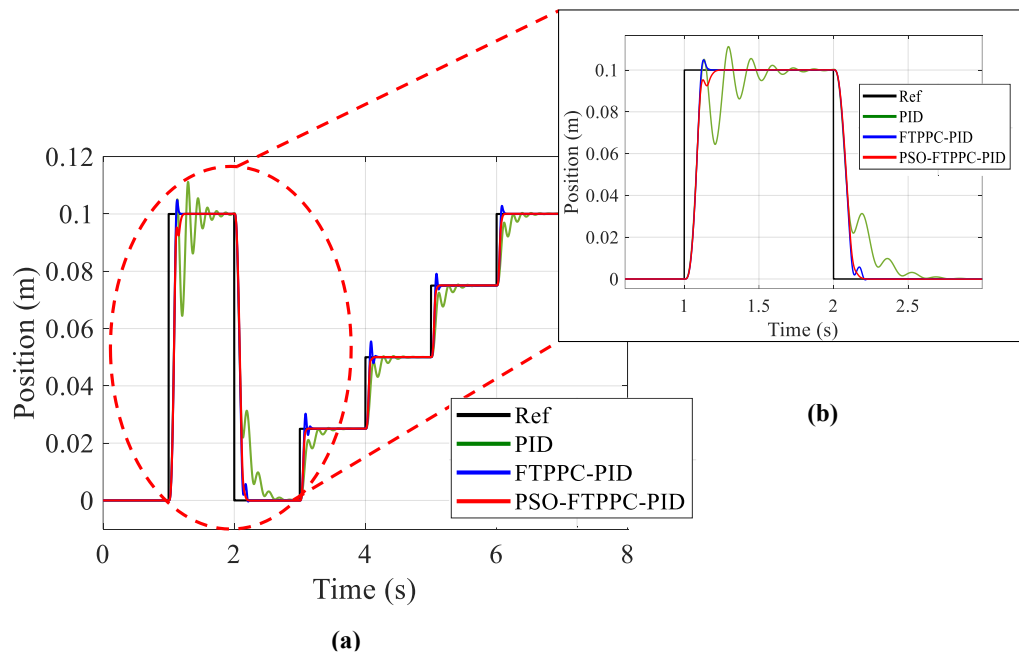


Fig. 5. Sample of multi-step displacement responses on PPDVC rod-piston position performances; comparison between PSO-FTPPC-PID, FTPPC-PID, and PID; (a) Overall time sample (b) Zoom-in view sample

The sample between 1-2 seconds in Fig. 9(b) clearly illustrates the difference in performance during the first changes in rod-piston displacement. The average time taken by the PPVDC with FTPPC-PID was 0.04 seconds faster than PSO-FTPPC-PID, resulting in overshoots in the rod-piston displacement as shown in Fig. 5. Fig. 10 displays the velocity and friction force, where PSO-FTPPC-PID demonstrates superior capability and sustains it at a specific level, achieving a static force at zero velocity (see Fig. 9). Although the pattern of results is similar for the PPVDC with FTPPC-PID, there are some minor overshoots. In contrast, the high-frequency oscillation in PPVDC with PID velocity affects the force friction, causing very oscillated forces on the rod-piston motion. Table 2 summarizes the robustness between the PSO-FTPPC-PID, FTPPC-PID, and PID control systems.

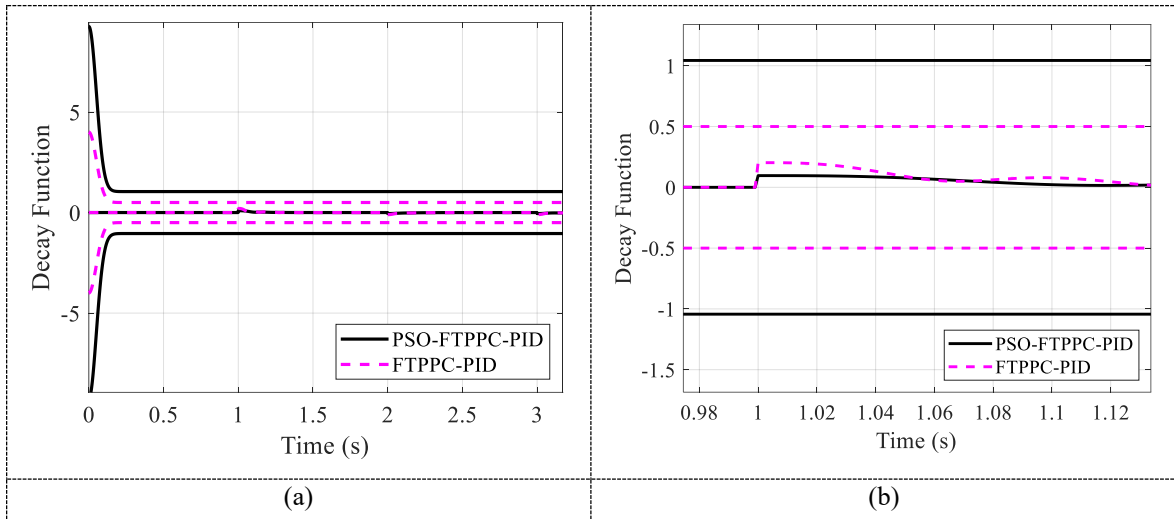


Fig. 6. Sample of Error transformation for both FTPPC-PID and PSO-FTPPC-PID in the Decay smooth function boundaries (a) Overall time sample (b) Zoom-in view sample

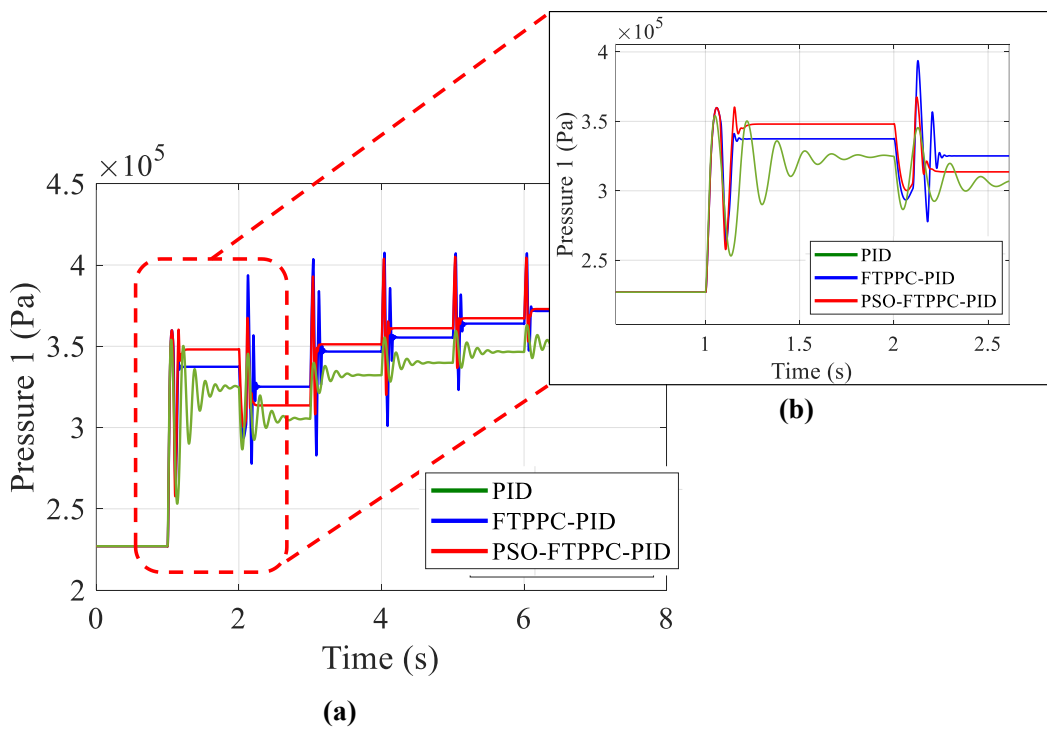


Fig. 7. Sample of pressure in Pressure 1 performances between PSO-FTPPC-PID, FTPPC-PID, and PID on PVDC; (a) Overall time sample (b) Zoom-in view sample

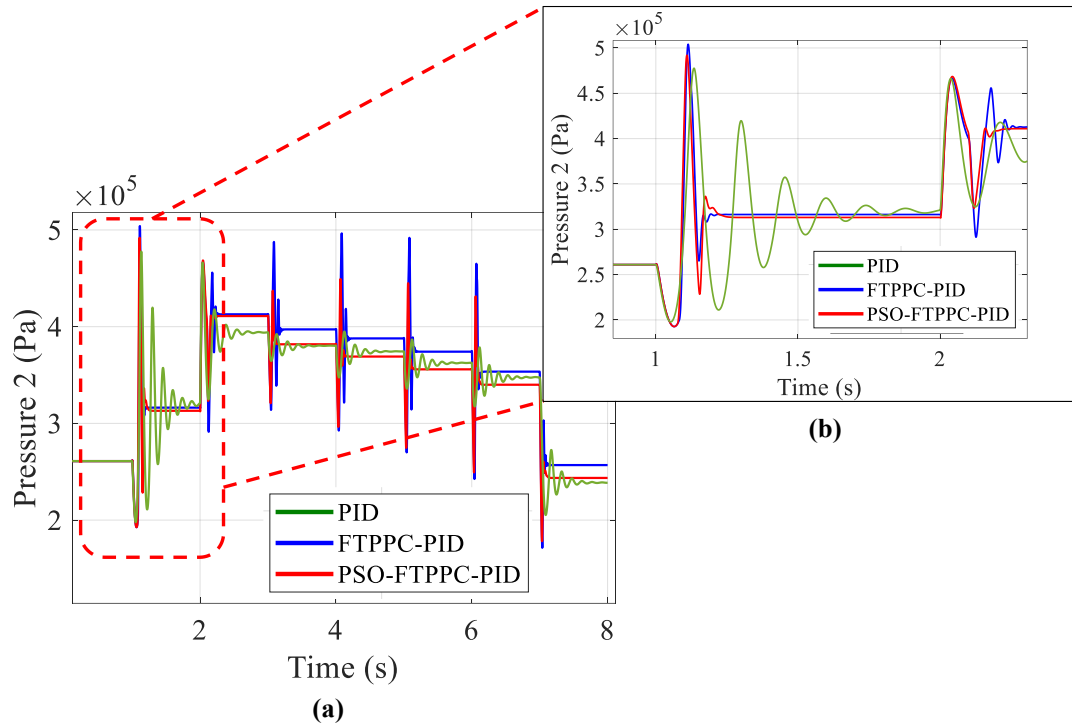


Fig. 8. Sample of pressure in Pressure 2 performances between PSO-FTTPC-PID, FTTPC-PID, and PID on PVDC; (a) Overall time sample (b) Zoom-in view sample

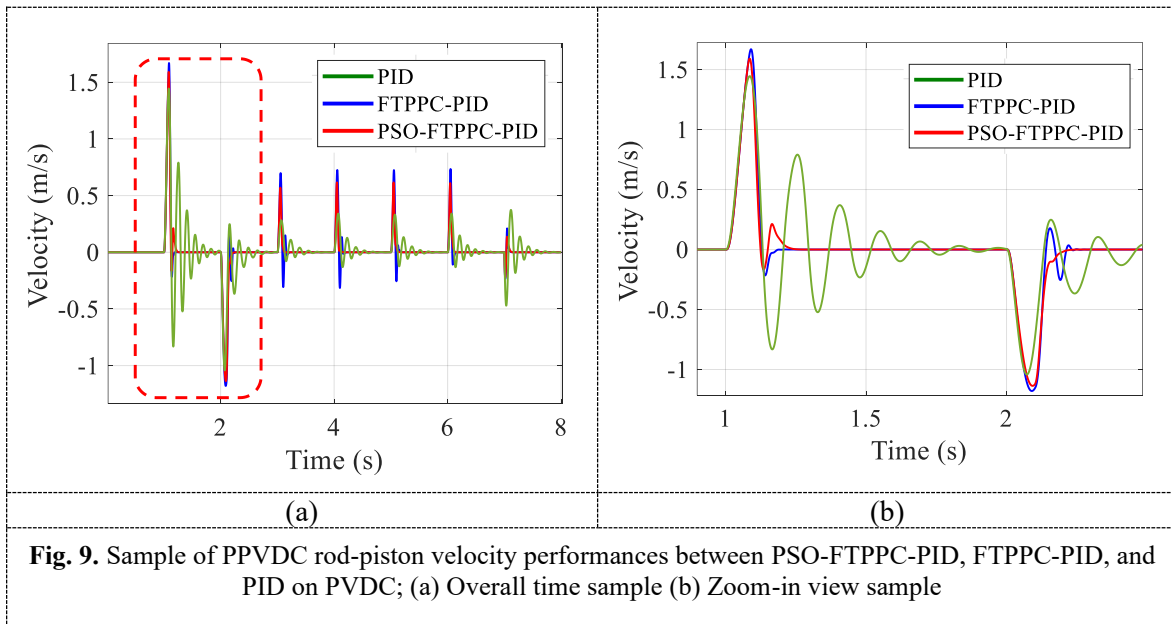
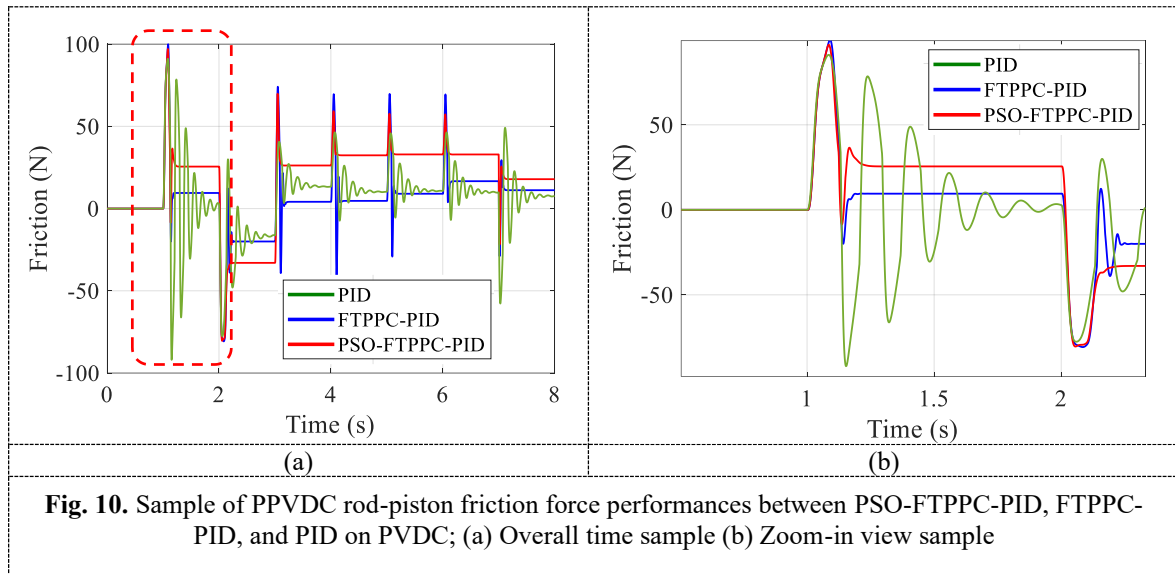


Fig. 9. Sample of PPVDC rod-piston velocity performances between PSO-FTTPC-PID, FTTPC-PID, and PID on PVDC; (a) Overall time sample (b) Zoom-in view sample

Table 2. Performance and robustness of the controllers

Performance	Controller		
	PID	FTTPC-PID	PSO-FTTPC-PID
Rise Time	0.0657s	0.0607s	0.0649s
Settling Time	0.6701s	0.1452s	0.1876s
Overshoot	11.0618mm	4.8929mm	0.0038mm



6. Conclusion

PSO-FTTPC-PID control system for PPVDC rod-piston position control for PPVDC of FTG robot was presented. The performance of this control system was compared to two other control systems: a conventional PID and a bang-bang-tuned FTTPC-PID. The comparison was conducted through simulations and analyses of the rod-piston positioning. The results showed that the PSO-FTTPC-PID outperformed both non-optimized controllers by providing a minimum steady-state error with almost no oscillation during the rising period, even though it was slightly slower in response compared to FTTPC-PID. Additionally, the PSO-FTTPC-PID stabilized the internal cylinder system, allowing for control of the internal frictional force by rapidly sustaining piston velocity and suppressing oscillation (dynamic frictional force to static frictional force). Internal friction can cause unstable pressure in chambers, leading to uncontrollable high overshoots during the first rising period of the rod-piston displacement. However, the PSO-FTTPC-PID can minimize this issue, leaving only one overshoot on the piston motion. This single low spike in pressures and velocity has no significant impact on the rod-piston displacement performance. In future work, the proposed PSO-FTTPC-PID will be applied to the actual PPVDC system, and modifications or improvements may be made based on hardware constraints and other uncertainties.

Author Contribution: All authors contributed equally to the main contributor to this paper. All authors read and approved the final paper.

Funding: This research received funding from the Ministry of Higher Education for providing financial support under Fundamental Research Grant Scheme (FRGS) No. FRGS/1/2019/TK04/UMP/02/1 (University reference RDU1901106).

Acknowledgement: The authors would like to thank the Ministry of Higher Education for providing financial support under Fundamental Research Grant Scheme (FRGS) No. FRGS/1/2019/TK04/UMP/02/1 (University reference RDU1901106) and Universiti Malaysia Pahang for laboratory facilities.

Conflicts of Interest: The authors declare no conflict of interest.

References

- [1] A. Madariaga, M. Cuesta, E. Dominguez, A. Garay, G. Ortiz-de-Zarate, and P. J. Arrazola, "Enhancing surface integrity of A7050-T7451 aluminium alloy by pneumatic machine hammer peening," *Procedia CIRP*, vol. 108, pp. 317-322, 2022, <https://doi.org/10.1016/j.procir.2022.03.053>.

-
- [2] D. Xie, Z. Ma, J. Liu, and S. Zuo, "Pneumatic Artificial Muscle Based on Novel Winding Method," *Actuators*, vol. 10, no. 5, p. 100, 2021, <https://doi.org/10.3390/act10050100>.
- [3] R. Singh and H. K. Verma, "Development of PLC-Based Controller for Pneumatic Pressing Machine in Engine-Bearing Manufacturing Plant," *Procedia Computer Science*, vol. 125, pp. 449-458, 2018, <https://doi.org/10.1016/j.procs.2017.12.059>.
- [4] Y. Wu *et al.*, "A bioinspired multi-knuckle dexterous pneumatic soft finger," *Sensors and Actuators A: Physical*, vol. 350, p. 114105, 2023, <https://doi.org/10.1016/j.sna.2022.114105>.
- [5] M. Yu *et al.*, "A self-sensing soft pneumatic actuator with closed-Loop control for haptic feedback wearable devices," *Materials & Design*, vol. 223, p. 111149, 2022, <https://doi.org/10.1016/j.matdes.2022.111149>.
- [6] G. Jin *et al.*, "Bioinspired soft caterpillar robot with ultra-stretchable bionic sensors based on functional liquid metal," *Nano Energy*, vol. 84, p. 105896, 2021, <https://doi.org/10.1016/j.nanoen.2021.105896>.
- [7] C. M. Ho, D. T. Tran, and K. K. Ahn, "Adaptive sliding mode control based nonlinear disturbance observer for active suspension with pneumatic spring," *Journal of Sound and Vibration*, vol. 509, p. 116241, 2021, <https://doi.org/10.1016/j.jsv.2021.116241>.
- [8] Z. Liu, X. Yin, K. Peng, X. Wang, and Q. Chen, "Soft pneumatic actuators adapted in multiple environments: A novel fuzzy cascade strategy for the dynamics control with hysteresis compensation," *Mechatronics*, vol. 84, p. 102797, 2022, <https://doi.org/10.1016/j.mechatronics.2022.102797>.
- [9] Z. Lin, Q. Wei, R. Ji, X. Huang, Y. Yuan, and Z. Zhao, "An Electro-Pneumatic Force Tracking System using Fuzzy Logic Based Volume Flow Control," *Energies*, vol. 12, no. 20, p. 4011, 2019. [Online]. Available: <https://www.mdpi.com/1996-1073/12/20/4011>.
- [10] H. Du, C. Hu, W. Xiong, Z. A. Jiang, and L. Wang, "Energy optimization of pneumatic actuating systems using expansion energy and exhaust recycling," *Journal of Cleaner Production*, vol. 254, p. 119983, 2020, <https://doi.org/10.1016/j.jclepro.2020.119983>.
- [11] Y. Wang, X.-J. Liu, and H. Zhao, "Speeding up soft pneumatic actuators through pressure and flow dynamics modeling and optimization," *Extreme Mechanics Letters*, vol. 57, p. 101914, 2022, <https://doi.org/10.1016/j.eml.2022.101914>.
- [12] M. I. P. Azahar, A. Irawan, and R. M. T. R. Ismail, "Self-tuning hybrid fuzzy sliding surface control for pneumatic servo system positioning," *Control Engineering Practice*, vol. 113, p. 104838, 2021, <https://doi.org/10.1016/j.conengprac.2021.104838>.
- [13] Y. Dai, Z. Deng, X. Wang, and H. Yuan, "A Hybrid Controller for a Soft Pneumatic Manipulator Based on Model Predictive Control and Iterative Learning Control," *Sensors*, vol. 23, no. 3, p. 1272, 2023. [Online]. Available: <https://www.mdpi.com/1424-8220/23/3/1272>.
- [14] A. Irawan and M. I. P. Azahar, "Cascade Control Strategy on Servo Pneumatic System with Fuzzy Self-Adaptive System," *Journal of Control, Automation and Electrical Systems*, vol. 31, no. 6, pp. 1412-1425, 2020, <https://doi.org/10.1007/s40313-020-00642-4>.
- [15] J. Wang, C. Shao, and Y.-Q. Chen, "Fractional order sliding mode control via disturbance observer for a class of fractional order systems with mismatched disturbance," *Mechatronics*, vol. 53, pp. 8-19, 2018, <https://doi.org/10.1016/j.mechatronics.2018.05.006>.
- [16] M. I. Putra, A. Irawan, and R. M. Taufika, "Fuzzy Self-Adaptive Sliding Mode Control for Pneumatic Cylinder Rod-Piston Motion Precision Control," in *Journal of Physics: Conference Series*, vol. 1532, 2020, <https://doi.org/10.1088/1742-6596/1532/1/012028>.
- [17] O. Ulkir, G. Akgun, A. Nasap, and E. Kaplanoglu, "Data-Driven Predictive Control of a Pneumatic Ankle Foot Orthosis," *Advances in Electrical and Computer Engineering*, vol. 21, pp. 65-74, 2021, <https://doi.org/10.4316/AECE.2021.01007>.
- [18] M. I. P. Azahar, A. Irawan, and R. M. Taufika, "Fuzzy Self-Adaptive PID for Pneumatic Piston Rod Motion Control," in *ICSGRC 2019 - 2019 IEEE 10th Control and System Graduate Research Colloquium, Proceeding*, pp. 82-87, 2019, <https://doi.org/10.1109/ICSGRC.2019.8837064>.
-

-
- [19] M. Al-Dhaifallah, N. Kanagaraj, and K. S. Nisar, "Fuzzy Fractional-Order PID Controller for Fractional Model of Pneumatic Pressure System," *Mathematical Problems in Engineering*, vol. 2018, p. 5478781, 2018, <https://doi.org/10.1155/2018/5478781>.
- [20] H. Ren, J. Fan, and O. Kaynak, "Optimal Design of a Fractional-Order Proportional-Integer-Differential Controller for a Pneumatic Position Servo System," *IEEE Transactions on Industrial Electronics*, vol. 66, no. 8, pp. 6220-6229, 2019, <https://doi.org/10.1109/TIE.2018.2870412>.
- [21] C. P. Bechlioulis and G. A. Rovithakis, "Robust Adaptive Control of Feedback Linearizable MIMO Nonlinear Systems With Prescribed Performance," *IEEE Transactions on Automatic Control*, vol. 53, no. 9, pp. 2090-2099, 2008, <https://doi.org/10.1109/TAC.2008.929402>.
- [22] Y. Liu and H. Chen, "Adaptive Sliding Mode Control for Uncertain Active Suspension Systems With Prescribed Performance," *IEEE Transactions on Systems, Man, and Cybernetics: Systems*, pp. 1-9, 2020, <https://doi.org/10.1109/TSMC.2019.2961927>.
- [23] S. Wang, J. Na, and Q. Chen, "Adaptive Predefined Performance Sliding Mode Control of Motor Driving Systems With Disturbances," *IEEE Transactions on Energy Conversion*, pp. 1-1, 2020, <https://doi.org/10.1109/TEC.2020.3038010>.
- [24] M. I. P. Azahar and A. Irawan, "Enhancing Precision on Pneumatic Actuator Positioning using Cascaded Finite-time Prescribed Performance Control," in *2021 11th IEEE International Conference on Control System, Computing and Engineering (ICCSCE)*, pp. 131-136, 2021, <https://doi.org/10.1109/ICCSCE52189.2021.9530956>.
- [25] A. Irawan, M. I. P. Azahar, and D. Pebrianti, "Interaction Motion Control on Tri-finger Pneumatic Grasper using Variable Convergence Rate Prescribed Performance Impedance Control with Pressure-based Force Estimator," *Journal of Robotics and Control (JRC)*, vol. 3, no. 5, pp. 716-724, 2022, <https://doi.org/10.18196/jrc.v3i5.16316>.
- [26] A. Kaveh, S. M. Hosseini, and A. Zaeerza, "A Physics-based Metaheuristic Algorithm Based on Doppler Effect Phenomenon and Mean Euclidian Distance Threshold," *Periodica Polytechnica Civil Engineering*, vol. 66, no. 3, pp. 820-842, 2022, <https://doi.org/10.3311/PPci.20133>
- [27] R. L. Haupt and S. E. Haupt, *Practical Genetic Algorithms*. Wiley, 2004, <https://doi.org/10.1002/0471671746>.
- [28] H.-J. Yang and X. Hu, "Wavelet neural network with improved genetic algorithm for traffic flow time series prediction," *Optik*, vol. 127, pp. 8103-8110, 2016, <https://doi.org/10.1016/j.ijleo.2016.06.017>.
- [29] M. A. Markom, A. H. Adom, S. A. A. Shukor, N. A. Rahim, E. S. M. M. Tan, and A. Irawan, "Scan matching and KNN classification for mobile robot localisation algorithm," in *2017 IEEE 3rd International Symposium in Robotics and Manufacturing Automation, ROMA 2017*, pp. 1-6, 2017, <https://doi.org/10.1109/ROMA.2017.8231836>.
- [30] E. W. Suseno and A. Ma'arif, "Tuning of PID Controller Parameters with Genetic Algorithm Method on DC Motor," *International Journal of Robotics and Control Systems*, vol. 1, no. 1, p. 13, 2021, <https://doi.org/10.31763/ijrcs.v1i1.249>.
- [31] M. M. Alam, A. Irawan, and T. Y. Yin, "Buoyancy effect control in multi legged robot locomotion on seabed using integrated impedance-fuzzy logic approach," *Indian Journal of Geo-Marine Sciences*, vol. 44, no. 12, pp. 1937-1945, 2015, <https://doi.org/10.1023/A:1008202821328>.
- [32] R. Storn and K. Price, "Differential Evolution – A Simple and Efficient Heuristic for global Optimization over Continuous Spaces," *Journal of Global Optimization*, vol. 11, no. 4, pp. 341-359, 1997, <https://doi.org/10.1109/4235.771163>.
- [33] Y. Xin, L. Yong, and L. Guangming, "Evolutionary programming made faster," *IEEE Transactions on Evolutionary Computation*, vol. 3, no. 2, pp. 82-102, 1999, <https://doi.org/10.1109/MHS.1995.494215>.
- [34] R. Eberhart and J. Kennedy, "A new optimizer using particle swarm theory," in *MHS'95. Proceedings of the Sixth International Symposium on Micro Machine and Human Science*, pp. 39-43, 1995, <https://doi.org/10.1109/CI-M.2006.248054>.
- [35] M. Dorigo, M. Birattari, and T. Stutzle, "Ant colony optimization," *Computational Intelligence Magazine, IEEE*, vol. 1, no. 4, pp. 28-39, 2006, <https://doi.org/10.1016/j.asoc.2007.05.007>.
-

- [36] D. Karaboga and B. Basturk, "On the performance of artificial bee colony (ABC) algorithm," *Applied Soft Computing*, vol. 8, no. 1, pp. 687-697, 2008, <https://doi.org/10.1016/j.asoc.2007.05.007>.
- [37] S. Mirjalili, S. M. Mirjalili, and A. Lewis, "Grey Wolf Optimizer," *Advances in Engineering Software*, vol. 69, pp. 46-61, 3// 2014, <http://dx.doi.org/10.1016/j.advengsoft.2013.12.007>.
- [38] S. Mirjalili, "Moth-flame optimization algorithm: A novel nature-inspired heuristic paradigm," *Knowledge-Based Systems*, vol. 89, pp. 228-249, 2015, <https://doi.org/10.1016/j.knsys.2015.07.006>.
- [39] M. H. Sulaiman, Z. Mustaffa, M. M. Saari, and H. Daniyal, "Barnacles Mating Optimizer: A new bio-inspired algorithm for solving engineering optimization problems," *Engineering Applications of Artificial Intelligence*, vol. 87, p. 103330, 2020, <https://doi.org/10.1016/j.engappai.2019.103330>.
- [40] M. H. Sulaiman, Z. Mustaffa, M. M. Saari, H. Daniyal, and S. Mirjalili, "Evolutionary mating algorithm," *Neural Computing and Applications*, vol. 35, no. 1, pp. 487-516, 2023, <https://doi.org/10.1007/s00521-022-07761-w>.
- [41] E. Rashedi, H. Nezamabadi-pour, and S. Saryazdi, "GSA: A Gravitational Search Algorithm," *Information Sciences*, vol. 179, no. 13, pp. 2232-2248, 2009, <https://doi.org/10.1016/j.ins.2009.03.004>.
- [42] K. S. Lee and Z. W. Geem, "A new meta-heuristic algorithm for continuous engineering optimization: harmony search theory and practice," *Computer Methods in Applied Mechanics and Engineering*, vol. 194, no. 36, pp. 3902-3933, 2005, <https://doi.org/10.1016/j.cma.2004.09.007>.
- [43] S. A. Celtek, A. Durdu, and M. E. M. Ali, "Real-time traffic signal control with swarm optimization methods," *Measurement*, vol. 166, p. 108206, 2020, <https://doi.org/10.1016/j.measurement.2020.108206>.
- [44] N. X. Chiem, N. D. Anh, A. D. Lukianov, P. D. Tung, H. D. Long, and N. D. Linh, "Design real-time embedded optimal PD fuzzy controller by PSO algorithm for autonomous vehicle mounted camera," *AIP Conference Proceedings*, vol. 2188, no. 1, 2019, <https://doi.org/10.1063/1.5138401>.
- [45] D. You, Y. Lei, S. Liu, Y. Zhang, and M. Zhang, "Networked Control System Based on PSO-RBF Neural Network Time-Delay Prediction Model," *Applied Sciences*, vol. 13, no. 1, p. 536, 2023, <https://doi.org/10.3390/app13010536>.
- [46] K. K. Pandey, C. Kumbhar, D. R. Parhi, S. K. Mathivanan, P. Jayagopal, and A. Haque, "Trajectory Planning and Collision Control of a Mobile Robot: A Penalty-Based PSO Approach," *Mathematical Problems in Engineering*, vol. 2023, p. 1040461, 2023, <https://doi.org/10.1155/2023/1040461>.
- [47] A. Saleem, B. Taha, T. Tutunji, and A. Al-Qaisia, "Identification and cascade control of servo-pneumatic system using Particle Swarm Optimization," *Simulation Modelling Practice and Theory*, vol. 52, pp. 164-179, 2015, <https://doi.org/10.1016/j.simpat.2015.01.007>.
- [48] M. Chavoshian, M. Taghizadeh, and M. Mazare, "Hybrid Dynamic Neural Network and PID Control of Pneumatic Artificial Muscle Using the PSO Algorithm," *International Journal of Automation and Computing*, vol. 17, no. 3, pp. 428-438, 2020, <https://doi.org/10.1007/s11633-019-1196-5>.
- [49] N. Ali, Y. Ayaz, and J. Iqbal, "Collaborative Position Control of Pantograph Robot Using Particle Swarm Optimization," *International Journal of Control, Automation and Systems*, vol. 20, no. 1, pp. 198-207, 2022, <https://doi.org/10.1007/s12555-019-0931-6>.
- [50] M. I. P. Azahar, A. Irawan, and M. S. Ramli, "Finite-Time Prescribed Performance Control for Dynamic Positioning of Pneumatic Servo System," in *2020 IEEE 8th Conference on Systems, Process and Control (ICSPC)*, pp. 1-6, 2020, <https://doi.org/10.1109/ICSPC50992.2020.9305755>.
- [51] A. Irawan, M. I. P. Azahar, and D. Pebrianti, "Interaction Motion Control on Tri-finger Pneumatic Grasper using Variable Convergence Rate Prescribed Performance Impedance Control with Pressure-based Force Estimator," *Journal of Robotics and Control (JRC)*, vol. 3, no. 5, p. 9, 2022, <https://doi.org/10.18196/jrc.v3i5.16316>.
- [52] A. Irawan, M. I. P. Azahar, and M. A. Hashimi, "Sensorless force estimation on fingertip with gravitational compensation for heavy-duty pneumatic tri-grasper robot," *IET Conference Proceedings*, pp. 1-5, <https://doi.org/10.1049/icp.2022.2483>.

- [53] M. Iskandar Putra, A. Irawan, and R. Mohd Taufika, "Fuzzy Self-Adaptive Sliding Mode Control for Pneumatic Cylinder Rod-Piston Motion Precision Control," *Journal of Physics: Conference Series*, vol. 1532, p. 012028, 2020, <https://doi.org/10.1088/1742-6596/1532/1/012028>.
- [54] M. Karpenko and N. Sepehri, "Design and experimental evaluation of a nonlinear position controller for a pneumatic actuator with friction," in *Proceedings of the 2004 American Control Conference*, vol. 6, pp. 5078-5083, 2004, <https://doi.org/10.23919/ACC.2004.1384656>.
- [55] C.-R. Rad and O. Hancu, "An improved nonlinear modelling and identification methodology of a servo-pneumatic actuating system with complex internal design for high-accuracy motion control applications," *Simulation Modelling Practice and Theory*, vol. 75, pp. 29-47, 2017, <https://doi.org/10.1016/j.simpat.2017.03.008>.